nature synthesis

Article

https://doi.org/10.1038/s44160-022-00219-w

# Electrochemical gold-catalysed biocompatible C($sp^2$)–C($sp$) coupling

Received: 23 June 2022

Accepted: 5 December 2022

Published online: 12 January 2023

Check for updates

Hao Liang, Yilitabaier Julaiti, Chuan-Gang Zhao & Jin Xie

Gold-catalysed oxidative coupling reactions often require strong oxidants because of the high redox potential of Au(I)/Au(III) (1.41 V versus the saturated calomel electrode), resulting in poor reaction economy and functional group compatibility. Here we report a dinuclear gold-catalysed C($sp^2$)–C($sp$) coupling reaction between structurally diverse alkynes and arylhydrazines under electrochemical conditions. This approach provides a practical oxidative C–C coupling reaction that avoids the use of synthetic oxidants and instead produces $H_2$. This method exhibits excellent functional group compatibility towards compounds such as alcohols, amines, sulfides and electron-rich arenes, which possess functional groups sensitive to oxidizing agents. This synthetic robustness is further shown by the successful late-stage modification of different kinds of alkynes tethered to biomolecules such as amino acids, peptides, nucleotides and saccharides. Mechanistic studies suggest a first aryl radical oxidative addition step with Au(I), followed by anodic oxidation to generate the highly electrophilic Ar–Au(III) species for subsequent σ-activation of alkynes.

Transition metal-catalysed carbon–carbon bond formation is one of the core components in organic synthesis and serves as the cornerstone for the facile construction of drugs and multifunctional materials[1]. In recent years, gold-catalysed oxidative carbon–carbon coupling has become an emerging synthetic method, but the high Au(I)/Au(III) redox potential of 1.41 V requires the use of strong synthetic oxidants to achieve such a change in valency[2–12]. Despite major efforts, the use of sacrificial oxidants in such reactions hardly supports the synthetic economy and functional group compatibility of gold-catalysed oxidative couplings. Consequently, the development of gold-catalysed C–C coupling in the absence of external oxidants has attracted considerable attention[13–32].

The alkyne motif is an important and versatile functional group in organic chemistry with which one can not only readily construct a rich library of organic compounds, but can also open a new door to target molecules that are widely useful in drug discovery and materials research (Fig. 1a)[33]. With the acidity of terminal alkynes, the construction of C($sp^3$)–C($sp$) bonds can be achieved by nucleophilic substitution or addition from terminal alkynes. The formation of the C($sp^2$)–C($sp$) bond is more challenging, and Pd/Cu co-catalysed Sonogashira coupling has emerged as the most effective strategy[34,35]. However, the high reactivity of palladium might compromise the functional group compatibility of these reactions and thus potentially limit their application. To overcome this inherent limitation, gold-catalysed oxidative C($sp^2$)–C($sp$) reactions have been developed, but with strong external oxidants, such as $PhI(OAc)_2$[36–42]. In the absence of external oxidants, gold-catalysed C($sp^2$)–C($sp$) couplings of either terminal alkynes or trimethylsilyl-protected alkynes with aryldiazonium salts were successfully developed as an important upgrade to previous approaches (Fig. 1b)[43–45]. While powerful, the aryldiazonium salts are strong electrophiles that accept electrons, thus there is an inherent limit to the redox-sensitive functional groups that can survive these conditions. Consequently, we wondered whether the aryl radical can be generated in situ from commercially available arylhydrazines under mild reaction conditions[46], avoiding the direct handling of explosive aryldiazonium salts for gold-catalysed C($sp^2$)–C($sp$) couplings.

Because electrochemical reactions can tune the oxidation process, they have been increasingly explored in transition metal-catalysed oxidative coupling[47–53]. In 2019, Shi et al.[54] realized the first electrochemical gold-catalysed C($sp$)–C($sp$) coupling of two different alkynes using C/

State Key Laboratory of Coordination Chemistry, Jiangsu Key Laboratory of Advanced Organic Materials, Chemistry and Biomedicine Innovation Center (ChemBIC), School of Chemistry and Chemical Engineering, Nanjing University, Nanjing, China. e-mail: xie@nju.edu.cn

https://doi.org/10.1038/s44160-022-00219-w

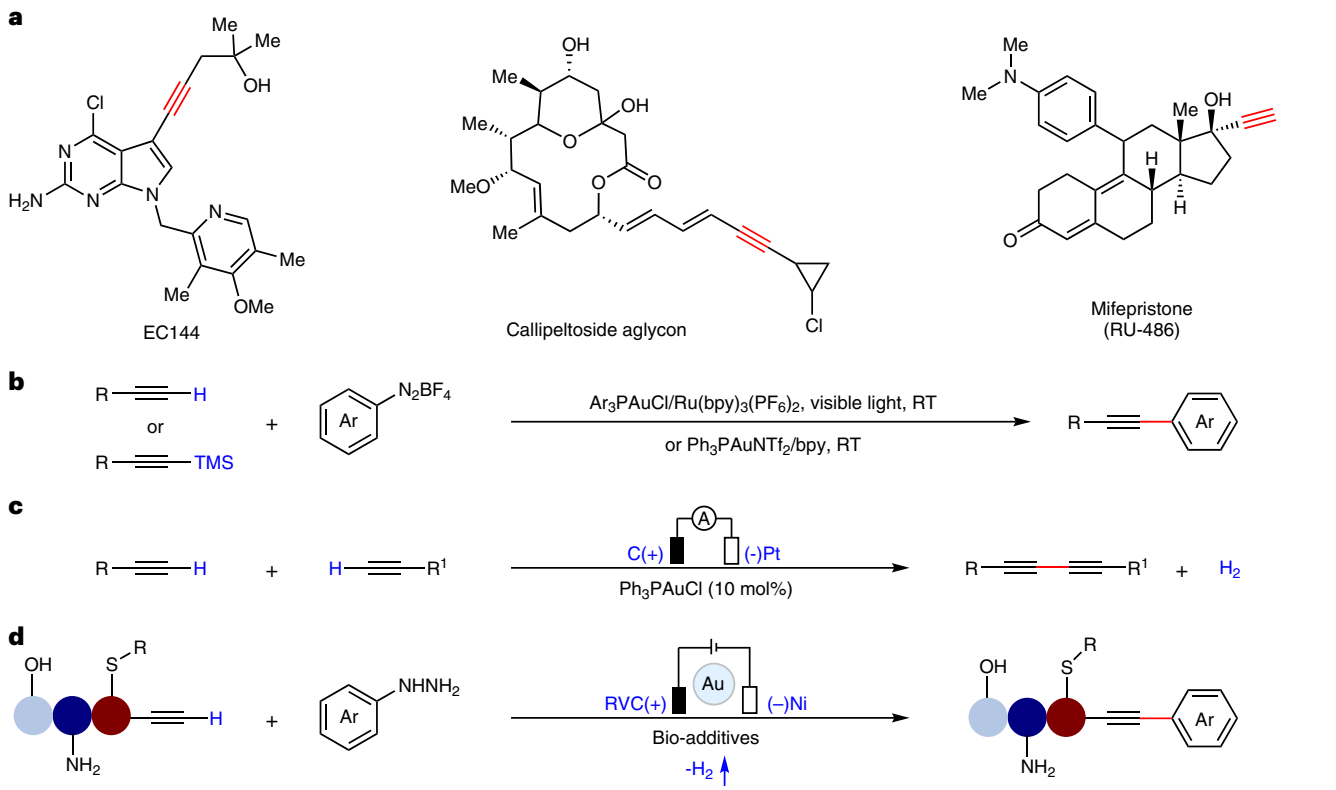


**Fig. 1 | The importance of alkynes in organic synthesis (appealing for gold-catalysed C($sp$)–C($sp^2$) coupling reactions and biocompatibility). a**, The alkyne motif as a representative functional group in biologically important molecules. **b**, Previous work on gold-catalysed C($sp^2$)–C($sp$) coupling with aryldiazonium salts[43,44,45]. The substrate compatibility is usually limited. **c**, The seminal work of Shi on electrochemical gold-catalysed C($sp$)–C($sp$) cross-coupling reactions without oxidants, showing the feasibility of gold-catalysed organic reactions under electrochemical conditions[54]. **d**, This work. Gold-catalysed biomolecule-compatible C($sp^2$)–C($sp$) coupling with $H_2$ evolution. A range of versatile functional groups and bio-additives are compatible in this electrochemical gold-catalysed coupling reaction. bpy, 2,2-bipyridine; RT, room temperature; RVC, reticulated vitreous carbon; Tf, trifluoromethylsulfonyl; TMS, trimethylsilyl.

Pt electrodes (Fig. 1c). Recently, the same group has reported an interesting C($sp^2$)–C($sp^2$) coupling between arylboronic acids and C($sp^2$)–C($sp$) coupling between arylboronic acids and terminal alkynes using C/Pt electrodes with air as the sole oxidant[55]. Following our continual interest in gold-catalysed coupling reactions[56–58], herein we report an electrochemical gold-catalysed C($sp^2$)–C($sp$) coupling of highly functionalized alkynes with arylhydrazines using inexpensive reticulated vitreous carbon/Ni electrodes with $H_2$ evolution (Fig. 1d). The hydrogen evolution supplants the use of oxidants and, when compared with its precedents, endows this protocol with an excellent functional group compatibility and chemoselectivity. Remarkably, the electrochemical reduction of Au(I) to Au(0) with hydrogen evolution is difficult to suppress in the absence of oxidants and we have found that the use of a gold-catalysed process with a matching anodic oxidation rate is an important factor.

## Optimization of reaction conditions

To initiate this study, the electron-rich 2-ethynylaniline (**1**) and 4-hydrazinylbenzonitrile (2) were selected as the model reaction to optimize the standard conditions (Table 1). Notably, 1,4-heteroatom-based (O, S, N) alkynes are prone to undergoing gold-catalysed cyclisation[59–61]. It was found that the desired coupling product (**3**) can be obtained in 63% yield with bis(diphenylphosphino)methane-$(AuCl)_2$ (dppm$(AuCl)_2$) (Fig. 2) as the gold catalyst in an ElectraSyn 2.0 cell (Table 1, entry 1). We envisioned that the additive 4,7-diphenyl-1,10-phenanthroline could serve as a transient ligand to stabilize the generated high-valency gold species[45]. Under these standard conditions, no cyclisation byproduct (**3′**) was formed and the free amino group—a very sensitive functional group in the presence of strong oxidants—was tolerated well. The use of dichloromethane or MeOH as solvents decreased the reaction efficiency (entries 2 and 3). The change of electrolyte from $n$-$Bu_4NOAc$ to $n$-$Bu_4NPF_6$ or $n$-$Bu_4NBF_4$ caused the yield of the desired C($sp^2$)–C($sp$) coupling reaction to be diminished, possibly because $n$-$Bu_4NOAc$ can stabilize the high-valence gold intermediate[54] (entries 4 and 5). The use of other gold complexes with the ligands shown in Fig. 2 decreased the reaction yield (entries 6–11). When a constant current of 9 mA was employed, a moderate yield of 44% was obtained (entry 12). In addition, it was found that when the cathode was replaced with platinum or graphite felt the reaction could not be promoted (entries 13 and 14). The control experiments show that the C($sp^2$)–C($sp$) coupling between 2-ethynylaniline (**1**) and 4-hydrazinylbenzonitrile (**2**) cannot occur in the absence of either the gold catalyst or the electric voltage (entries 15 and 16).

## Reaction scope

With the established reaction conditions (Table 1, entry 1) in hand, we investigated the scope of the reaction. As shown in Table 2, both aromatic alkynes and aliphatic alkynes are generally competent coupling partners in the electrochemical gold-catalysed C($sp^2$)–C($sp$) coupling. For the aromatic alkynes, both electron-rich and electron-poor functional groups on the phenyl groups tolerated the reaction conditions well, leading to the production of desired products (**4**–**14**) in satisfactory yields. Versatile halogens, such as Br (**7**) remain unaffected during the coupling process and could provide a platform for downstream modification. Importantly, we found that a wide range

https://doi.org/10.1038/s44160-022-00219-w

**Table 1 | Optimization of reaction conditions**

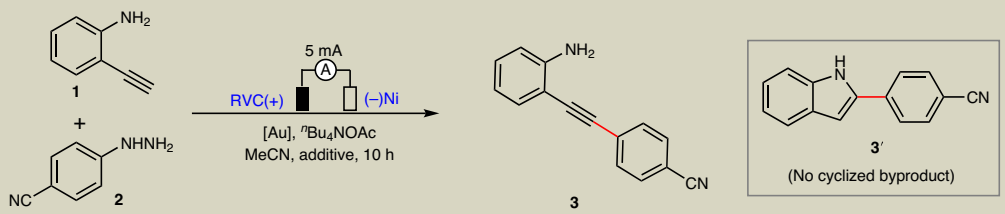


| Entry | Electrolyte | Gold catalyst (10 mol%) | Solvent | Yield (%)[a] |
|---|---|---|---|---|
| 1 | $^{n}Bu_4NOAc$ | $dppm(AuCl)_2$ | MeCN | 63 |
| 2 | $^{n}Bu_4NOAc$ | $dppm(AuCl)_2$ | $CH_2Cl_2$ | 12 |
| 3 | $^{n}Bu_4NOAc$ | $dppm(AuCl)_2$ | MeOH | Trace |
| 4 | $^{n}Bu_4NPF_6$ | $dppm(AuCl)_2$ | MeCN | Trace |
| 5 | $^{n}Bu_4NBF_4$ | $dppm(AuCl)_2$ | MeCN | 15 |
| 6 | $^{n}Bu_4NOAc$ | $dppm(AuOTs)_2$ | MeCN | 25 |
| 7 | $^{n}Bu_4NOAc$ | $dppe(AuCl)_2$ | MeCN | 33 |
| 8 | $^{n}Bu_4NOAc$ | $BINAP(AuCl)_2$ | MeCN | 11 |
| 9 | $^{n}Bu_4NOAc$ | XPhosAuCl | MeCN | 9 |
| 10 | $^{n}Bu_4NOAc$ | IPrAuCl | MeCN | 8 |
| 11 | $^{n}Bu_4NOAc$ | $dppp(AuCl)_2$ | MeCN | 18 |
| 12[b] | $^{n}Bu_4NOAc$ | $dppm(AuCl)_2$ | MeCN | 44 |
| 13[c] | $^{n}Bu_4NOAc$ | $dppm(AuCl)_2$ | MeCN | 57 |
| 14[d] | $^{n}Bu_4NOAc$ | $dppm(AuCl)_2$ | MeCN | 35 |
| 15 | $^{n}Bu_4NOAc$ | None | MeCN | ND |
| 16[e] | $^{n}Bu_4NOAc$ | $dppm(AuCl)_2$ | MeCN | ND |

[a]The isolated yield is shown. [b]Constant current of 9 mA. [c]Pt as cathode. [d]Graphite felt as the cathode. [e]No current. Reaction conditions: gold catalyst (10 mol%), **1** (0.3 mmol), **2** (1.5 mmol), 4,7-diphenyl-1,10-phenanthroline (40 mol%), 2,6-di-*tert*-butylpyridine (1.5 equiv.), *n*-$Bu_4NOAc$ (1.2 mmol) and MeCN (3 ml) in an ElectraSyn 2.0 cell with a constant current of 5 mA and ambient temperature for 10 h. ND, none detected; BINAP, 1,1′-binaphthyl-2,2′-diphemyl phosphine; dppe, 1,2-bis(diphenylphosphino)ethane; dppp, 1,3-bis(diphenylphosphino)propane; XPhos, 2-(dicyclohexylphosphino)-2′,4′,6′-tri(isopropyl)biphenyl.

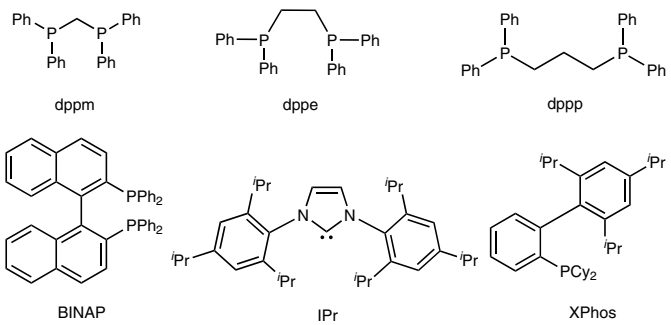


**Fig. 2 | Different ligands for the gold catalysts.** Cy, cyclohexyl; $^{i}$Pr, isopropyl.

of electron-rich 2-ethynylanilines can undergo this electrolytic coupling, giving rise to the expected products (**15**–**22**) in 55–69% yield. The relatively oxidant-sensitive sulfide can also be tolerated under mild conditions and delivers the coupling product (**23**) in 60% yield. The success of these electron-rich anilines and oxidant-sensitive sulfides shows the excellent functional group tolerance of this protocol, which is difficult to realize in the presence of external oxidants. Alkynes with heteroaromatic rings, such as thiophene (**13**) and pyridine (**14**) are also good coupling partners.

Subsequently, the reactions of a broad range of aliphatic alkynes were examined under the optimal conditions. It was found that a three-membered ring can tolerate the conditions well, affording the product (**25**) in 45% yield. Interestingly, hydroxyl-tethered aliphatic alkynes can smoothly undergo the expected C($sp^2$)–C($sp$) coupling to furnish products (**27**, **28** and **33**–**38**) in moderate yields. It was found that hydroxyl groups at C4, C5 and C6 are compatible with the reaction and are retained because these products (**33**–**38**) do not further convert into the corresponding ethers, showing the tolerance of hydroxyl groups in the reaction. A series of useful functional groups, such as ester (**29**) and acetal (**30** and **31**) remain intact during the oxidative coupling. A conjugated enyne is a suitable coupling partner and affords the desired product (**32**) in 48% yield.

This electrochemical gold-catalysed C($sp^2$)–C($sp$) coupling protocol was applied to a series of complex alkynes. It was found that the reaction enjoys good functional group compatibility, and a variety of alkynes with different frameworks tolerate the conditions well, giving rise to the target products (**39**–**44**) in moderate yields. Regarding the scope of aromatic hydrazines, we found that hydrazines with *para* substituents such as halogen (**45** and **46**), electron-rich methoxy (**47**), electron-deficient trifluoromethyl (**48**) and ester groups (**49** and **50**) are all competent substrates. These same functional groups at the *meta* or *ortho* positions were found to have little influence on the reaction efficiency, affording the products (**51**–**56**) in synthetically acceptable yields.

## Late-stage modification of complex alkynes

After obtaining these results, we carried out gold-catalysed coupling reactions with a series of complex alkynes bearing several biomolecular

https://doi.org/10.1038/s44160-022-00219-w

**Table 2 | Reaction scope of gold-catalysed C($sp^2$)–C($sp$) coupling**

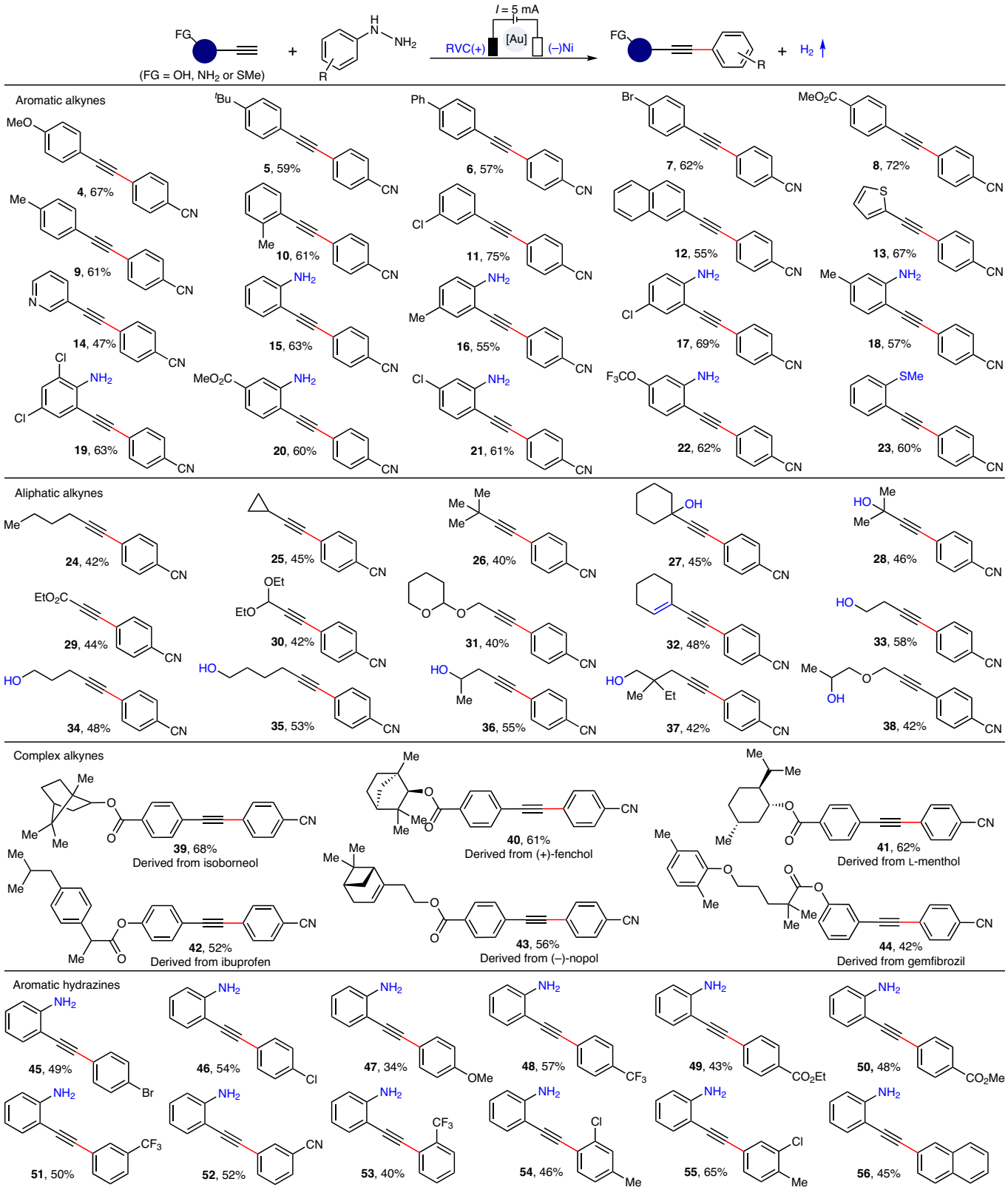


Standard conditions: dppm(AuCl)$_2$ (10 mol%), alkyne (0.3 mmol), arylhydrazines (1.5 mmol), 4,7-diphenyl-1,10-phenanthroline (40 mol%), *n*-Bu$_4$NOAc (1.2 mmol), 2,6-di-*tert*-butylpyridine (1.5 equiv.) and MeCN (3 ml) in an ElectraSyn 2.0 cell at a constant current of 5 mA and room temperature for 10 h.

https://doi.org/10.1038/s44160-022-00219-w

**Table 3 | Substrate scope of biomolecule-tethered alkynes**

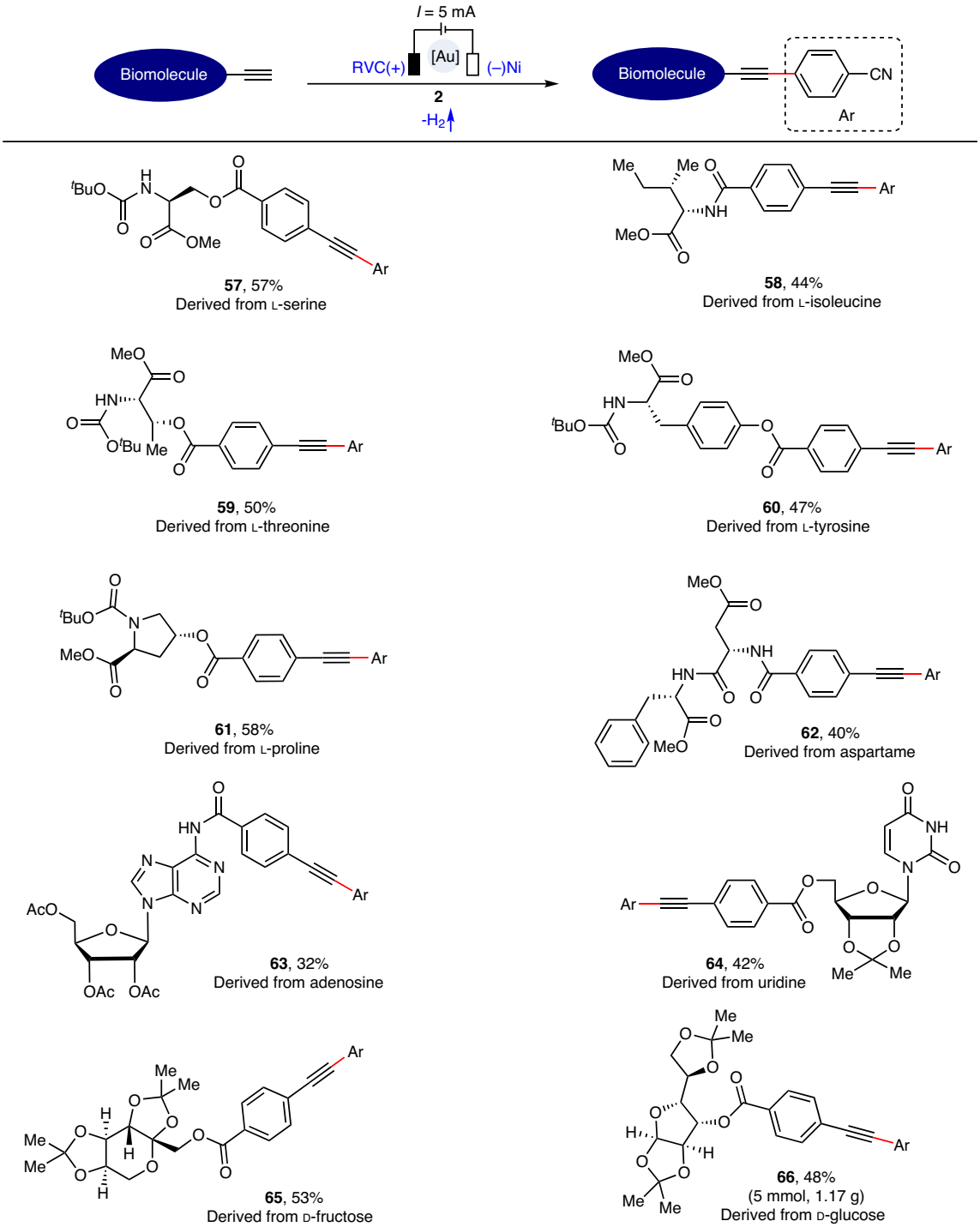


Standard conditions: dppm(AuCl)$_2$ (10 mol%), biomolecule-derived alkynes (0.3 mmol), hydrazines **2** (1.5 mmol), 4,7-diphenyl-1,10-phenanthroline (40 mol%), *n*-Bu$_4$NOAc (1.2 mmol), 2,6-di-*tert*-butylpyridine (1.5 equiv.) and MeCN (3 ml) in an ElectraSyn 2.0 cell at a constant current of 5 mA and room temperature for 10 h.

skeletons (Table 3) and found that amino acid-derived alkynes can uniformly undergo the expected C($sp^2$)–C($sp$) coupling, producing the products (**57**–**62**) in yields of 40–58%. When the derivatives of adenosine (**63**) and uridine (**64**) were added to the reaction, these nitrogen-containing alkynes tolerated the electrochemical reaction conditions well. Saccharide-containing alkynes are also efficient substrates in this gold-catalysed electrochemical C($sp^2$)–C($sp$) coupling and afford the products **65** and **66** in moderate yields. To demonstrate the scalability of this gold-catalysed coupling reaction, we completed the reaction on a 5 mmol scale, giving the expected product (**66**) in 48% yield (1.17 g).

## Investigation of the compatibility of bio-additives

As shown in Table 3, it was found that this gold-catalysed coupling has good functional group compatibility, and we questioned whether it can tolerate different kinds of biochemically important molecules[62–64].

https://doi.org/10.1038/s44160-022-00219-w

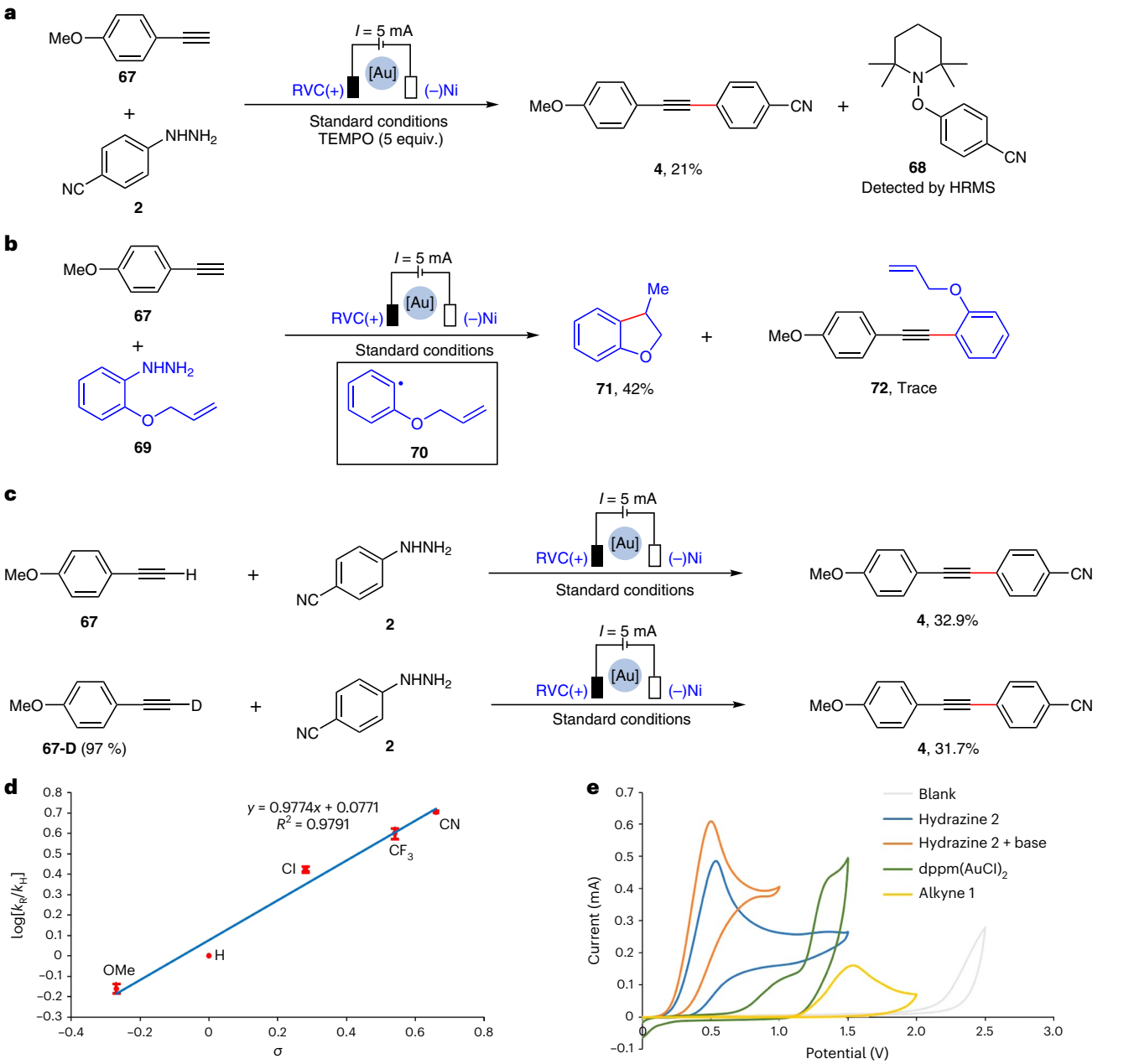


**Fig. 3 | Mechanistic studies.** Standard conditions: dppm$(AuCl)_2$ (10 mol%), alkyne (0.3 mmol), hydrazines (1.5 mmol), 4,7-diphenyl-1,10-phenanthroline (40 mol%), 2,6-di-*tert*-butylpyridine (1.5 equiv.), *n*-$Bu_4NOAc$ (1.2 mmol) and MeCN (3 ml) in an ElectraSyn 2.0 cell at a constant current of 5 mA and room temperature for 10 h. **a**, Radical trapping experiment. TEMPO (5 equiv.) was added to the reaction of **67** and **2** under standard conditions and the trapped product **68** was detected by high-resolution mass spectrometry (HRMS). **b**, Radical cyclisation experiment. Hydrazine **69** was subjected to standard conditions, and the five-membered cyclisation product **71** was obtained. **c**, Parallel kinetic isotope effect experiment. 1-ethynyl-4-methoxybenzene (**67**) and D-1-ethynyl-4-methoxybenzene (**67-D**) were employed under standard conditions, respectively. With a reaction time of 4 h, the kinetic isotope effect was calculated as 1.04. **d**, Hammett plot of substituted hydrazine derivatives. The electronic effect of different substituents on the reaction rate was examined in three parallel experiments. $k_R$, reaction rate constants with benzene ring bearing different substituents; $k_H$, reaction rate constant without substituent on the benzene ring. **e**, Cyclic voltammetry experiments. $Ag/Ag^+$ (Ag wire in 0.01 M $AgNO_3$ with 0.1 M *n*$Bu_4NOAc$ in $CH_3CN$) was used as the reference electrode at a scan rate of 100 mV $s^{-1}$, $E_p$, peak potential.

When a series of bio-additives, such as monosaccharides, amino acids, peptides, adenosine triphosphate, biotin and nucleotides were added to the reaction, they were found to influence the reaction very little and could still be detected when the coupling process was complete. Besides these small molecules, when some core macromolecules in organisms, such as DNA, RNA, albumin, chlorophyll, starch and enzymes were included as bio-additives in the gold-catalysed C($sp^2$)–C($sp$) coupling, the desired coupling products (**3**) were obtained in satisfactory yields (Table 4). These experiments suggest the possible biocompatibility of the gold-catalysed electrochemical reaction system towards a series of bio-additives.

## Reaction mechanism

To gain evidence that the mechanism of the gold-catalysed electrochemical C($sp^2$)–C($sp$) coupling is or is not a radical pathway, 2,2,6,6-tetramethyl-1-piperidinyloxy (TEMPO) was added to the

https://doi.org/10.1038/s44160-022-00219-w

**Table 4 | Investigation of the compatibility of bio-additives in the reaction**

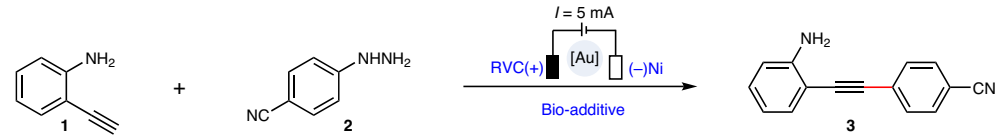


| Bio-additive | Yield | Bio-additive | Yield |
|---|---|---|---|
| 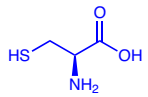 L-Cysteine (1 equiv.) | 54% | 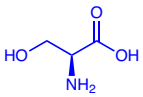 L-Serine (1 equiv.) | 55% |
| 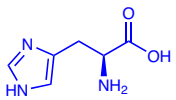 L-Histidine (1 equiv.) | 62% | 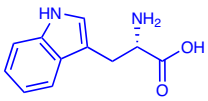 L-Tryptophan (1 equiv.) | 57% |
| 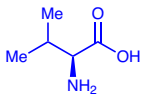 L-Valine (1 equiv.) | 60% | 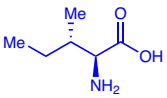 L-Isoleucine (1 equiv.) | 59% |
| 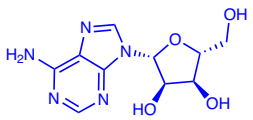 Adenosine (1 equiv.) | 57% | 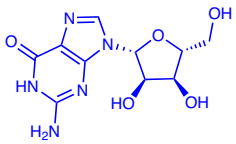 Guanosine (1 equiv.) | 56% |
| 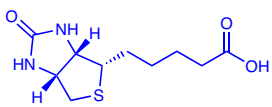 Biotin (1 equiv.) | 61% | 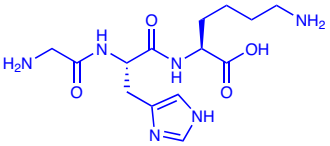 Copper peptide (1 equiv.) | 55% |
| 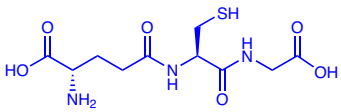 Glutathione (1 equiv.) | 59% | 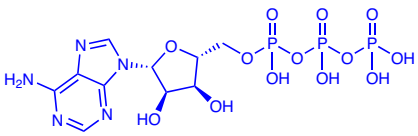 ATP (1 equiv.) | 56% |
| 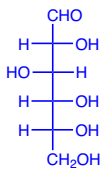 D-Glucose (1 equiv.) | 55% | Starch (10 mg ml$^{-1}$) | 60% |
| | | DNA (10 mg ml$^{-1}$) | 57% |
| | | RNA (10 mg ml$^{-1}$) | 55% |
| Chlorophyll (10 mg ml$^{-1}$) | 60% | Casein (10 mg ml$^{-1}$) | 60% |
| Bovine serum albumin (10 mg ml$^{-1}$) | 61% | Porcine trypsin (10 mg ml$^{-1}$) | 57% |

Reaction conditions: dppm(AuCl)$_2$ (10 mol%), alkyne 1 (0.3 mmol), hydrazines 2 (1.5 mmol), 4,7-diphenyl-1,10-phenanthroline (40 mol%), 2,6-di-*tert*-butylpyridine (1.5 equiv.), *n*-Bu$_4$NOAc (1.2 mmol), MeCN (3 ml) and bio-additive in an ElectraSyn 2.0 cell at a constant current of 5 mA and room temperature for 10 h. After the reaction finished, the reaction mixture was analysed and the isolated yield is shown. ATP, adenosine triphosphate.

reaction of 4-hydrazinylbenzonitrile (**2**) with 1-ethynyl-4-methoxybenzene (**67**) (Fig. 3a). It was shown by high-resolution mass spectrometry analysis that the corresponding aryl radical was successfully trapped by TEMPO, with the reaction yield dramatically decreasing to 21%. As shown in Fig. 3b, when the arylhydrazine (**69**) containing an alkene tethered at the *ortho* position was subjected to the standard conditions, a cyclized five-membered ring product (**71**) was produced in 42% yield, possibly owing to the formation of aryl radical intermediate (**70**) in

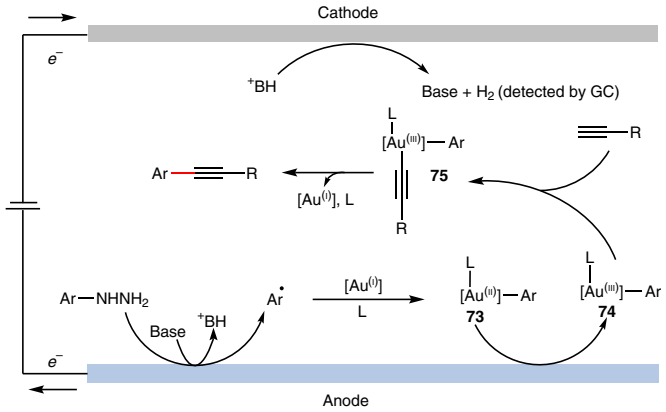


**Fig. 4 | Proposed reaction mechanism.** First, aryl radical oxidation addition with Au(I) to form Ar–Au(II) **73** and subsequent anodic oxidation generates the highly electrophilic Ar–Au(III) species **74**, which is able to proceed via σ activation of alkynes to produce **75**. Rapid reductive elimination from the Au(III) intermediate **75** gives rise to the final C($sp^2$)–C($sp$) product. Base, 2,6-di-*tert*-butylpyridine; GC, gas chromatography; L, 4,7-diphenyl-1,10-phenanthroline.

situ. These results would imply that a radical process is very likely. As shown in Fig. 3c, the parallel kinetic isotope effect experiments using 1-ethynyl-4-methoxybenzene (**67**) and D-1-ethynyl-4-methoxybenzene (**67-D**), respectively, suggested that the activation of the alkyne hydrogen bond might not be the rate-limiting step. Additionally, because no homocoupling byproducts of terminal alkynes were detected in these reactions, the direct σ activation of terminal alkyne with the gold(I) catalyst would be less likely (see Supplementary Fig. 29). The electronic effect of the hydrazine derivatives (such as 4-OMe, 4-Cl, 4-$CF_3$ and 4-CN) on the reaction rate was further verified by Hammett studies (Fig. 3d). The positive slope ($\rho$ = 0.9774) in the Hammett plot might suggest that electron-deficient aryl intermediates would be more favourable during the oxidation addition to the gold catalyst. As illustrated in Fig. 3e, the cyclic voltammetry experiments show that the oxidation potential of phenylhydrazine (**2**) is about +0.53 V (versus Ag/$AgNO_3$) but it is slightly lower at +0.50 V (versus Ag/$AgNO_3$) after the addition of a base. This change would suggest that the base may promote the oxidation of phenylhydrazine by accelerating the hydrogen transfer. It was also concluded that the gold catalyst employed has two obvious oxidation peaks, the first being $Au^I/Au^{II}$ ($E_p$ = +1.06 V versus Ag/$AgNO_3$) and the second being $Au^{II}/Au^{III}$ ($E_p$ = +1.41 V versus Ag/$AgNO_3$). This makes it possible for the aryl radical generated in situ from phenylhydrazine by anodic oxidation to recombine with the $Au^I$ catalyst.

These observations led to a plausible mechanism proposed in Fig. 4. With the assistance of a base, aromatic hydrazines are able to undergo oxidation at the anode to form a highly electrophilic aryl radical[46] that can recombine with the Au(I) catalyst to form an intermediate (**73**) in which the 4,7-diphenyl-1,10-phenanthroline ligand further stabilizes the high-valence gold species. Single-electron oxidation of this intermediate (**74**) generates Ar–Au(III), which would activate the terminal alkynes in a σ activation manner[65]. Finally, rapid reductive elimination from the high-valence gold species (**75**) delivers the expected C($sp^2$)–C($sp$) coupling products. To maintain the electronic balance during the reaction process, the protonated base ($HB^+$) is possibly reduced at the cathode to produce $H_2$, which can be detected by gas chromatography, and the base is regenerated.

## Discussion

We have developed a dinuclear gold-catalysed C($sp^2$)–C($sp$) coupling reaction of good compatibility under electrochemical conditions with cheap reticulated vitreous carbon/Ni electrodes. A wide range of structurally diverse alkynes can selectively couple with aromatic hydrazines. The good compatibility of this protocol towards oxidant-sensitive functional groups and bio-additives makes it promising for the construction of C($sp^2$)–C($sp$) bonds in complex alkynes. The use of electrochemical redox conditions allows for a sustainable gold-catalysed oxidative C–C coupling without the use of external synthetic oxidants, but instead by the formation of $H_2$. This protocol represents an important step forward towards gold-catalysed bioadditive-compatible oxidative C($sp^2$)–C($sp$) coupling in a sustainable manner.

## Methods

### General procedure for electrochemical gold-catalysed coupling

To an ElectraSyn undivided cell (10.0 ml) equipped with a stirring bar, dppm$(AuCl)_2$ (0.03 mmol; 10 mol%), alkyne (0.30 mmol; 1.0 equiv.), hydrazine (1.50 mmol; 5.0 equiv.), $n$$Bu_4$NOAc (1.20 mmol; 4.0 equiv.) and 4,7-diphenyl-1,10-phenanthroline (0.12 mmol; 40 mol%) are successively added. Then, $CH_3CN$ (3.0 ml) and 2,6-di-*tert*-butylpyridine (0.45 mmol; 1.5 equiv.) are added with a syringe. The ElectraSyn vial cap equipped with an anode (reticulated vitreous carbon; 4.0 cm × 0.6 cm × 0.6 cm) and a cathode (nickel foam; 4.0 cm × 0.8 cm × 0.2 cm) is inserted into the reaction mixture solution. The reaction mixture is then stirred and electrolysed at a constant current of 5 mA at room temperature for 10 h. After completion of the reaction, the solvent is removed under reduced pressure and the resulting residue is purified by flash column chromatography on silica gel to afford the desired product.

## Data availability

All of the data supporting the findings of this study are available within the article and its Supplementary Information files. Source data are provided with this paper.

## References

1. Ritleng, V., Sirlin, C. & Pfeffer, M. Ru-, Rh-, and Pd-catalyzed C–C bond formation involving C–H activation and addition on unsaturated substrates: reactions and mechanistic aspects. *Chem. Rev.* **102**, 1731–1770 (2002).
2. Hashmi, A. S. K. Gold-catalyzed organic reactions. *Chem. Rev.* **107**, 3180–3211 (2007).
3. Zhang, G., Peng, Y., Cui, L. & Zhang, L. Gold-catalyzed homogeneous oxidative cross-coupling reactions. *Angew. Chem. Int. Ed. Engl.* **48**, 3112–3115 (2009).
4. Wang, Q., Rudolph, M., Rominger, F. & Hashmi, A. S. K. Gold-catalyzed intermolecular oxidative diyne cyclizations via 1,6-carbene transfer. *Adv. Synth. Catal.* **362**, 755–759 (2020).
5. Ball, L. T., Lloyd-Jones, G. C. & Russell, C. A. Gold-catalyzed direct arylation. *Science* **337**, 1644–1648 (2012).
6. Ball, L. T., Lloyd-Jones, G. C. & Russell, C. A. Gold-catalyzed oxidative coupling of arylsilanes and arenes: origin of selectivity and improved precatalyst. *J. Am. Chem. Soc.* **136**, 254–264 (2014).
7. Banerjee, S., Bhoyare, V. W. & Patil, N. T. Gold and hypervalent iodine(III) reagents: liaisons over a decade for electrophilic functional group transfer reactions. *Chem. Commun.* **56**, 2677–2690 (2020).
8. Rocchigiani, L. & Bochmann, M. Recent advances in gold(III) chemistry: structure, bonding, reactivity, and role in homogeneous catalysis. *Chem. Rev.* **121**, 8364–8451 (2021).
9. Liu, K., Li, N., Ning, Y., Zhu, C. & Xie, J. Gold-catalyzed oxidative biaryl cross-coupling of organometallics. *Chem.* **5**, 2718–2730 (2019).
10. Li, W. et al. Cooperative Au/Ag dual-catalyzed cross-dehydrogenative biaryl coupling: reaction development and mechanistic insight. *J. Am. Chem. Soc.* **141**, 3187–3197 (2019).

11. Ye, X. et al. Gold-catalyzed oxidative coupling of alkynes toward the synthesis of cyclic conjugated diynes. *Chem.* **4**, 1983–1993 (2018).
12. Peng, H. et al. Gold-catalyzed oxidative cross-coupling of terminal alkynes: selective synthesis of unsymmetrical 1,3-diynes. *J. Am. Chem. Soc.* **136**, 13174–13177 (2014).
13. Wang, W. et al. Dinuclear gold catalysis. *Chem. Soc. Rev.* **50**, 1874–1912 (2021).
14. Zhang, L. et al. Reductive C–C coupling by desulfurizing gold-catalyzed photoreactions. *ACS Catal.* **9**, 6118–6123 (2019).
15. Hopkinson, M. N., Tlahuext-Aca, A. & Glorius, F. Merging visible light photoredox and gold catalysis. *Acc. Chem. Res.* **49**, 2261–2272 (2016).
16. Akram, M. O., Banerjee, S., Saswade, S. S., Bedi, V. & Patil, N. T. Oxidant-free oxidative gold catalysis: the new paradigm in cross-coupling reactions. *Chem. Commun.* **54**, 11069–11083 (2018).
17. Huang, L., Rudolph, M., Rominger, F. & Hashmi, A. S. K. Photosensitizer-free visible light-mediated gold-catalyzed 1,2-difunctionalization of alkynes. *Angew. Chem. Int. Ed.* **55**, 4808–4813 (2016).
18. Huang, L., Rominger, F., Rudolph, M. & Hashmi, A. S. K. A general access to organogold(III) complexes by oxidative addition of diazonium salts. *Chem. Commun.* **52**, 6435–6438 (2016).
19. Witzel, S., Sekine, K., Rudolph, M. & Hashmi, A. S. K. New transmetalation reagents for the gold-catalyzed visible light-enabled C($sp$ or $sp^2$)–C($sp^2$) cross-coupling with aryldiazonium salts in the absence of a photosensitizer. *Chem. Commun.* **54**, 13802–13804 (2018).
20. Taschinski, S. et al. Light-induced mechanistic divergence in gold(I) catalysis: revisiting the reactivity of diazonium salts. *Angew. Chem. Int. Ed.* **58**, 16988–16993 (2019).
21. Eppel, D., Rudolph, M., Rominger, F. & Hashmi, A. S. K. Mercury-free synthesis of pincer [C^N^C] $Au^{III}$ complexes by an oxidative addition/C–H activation cascade. *ChemSusChem* **13**, 1986–1990 (2020).
22. Zhang, L., Si, X., Rominger, F. & Hashmi, A. S. K. Visible-light-induced radical carbocyclization/*gem*-diborylation through triplet energy transfer between a gold catalyst and aryl iodides. *J. Am. Chem. Soc.* **142**, 10485–10493 (2020).
23. Si, X. et al. Visible light induced α-C($sp^3$)–H acetalization of saturated heterocycles catalyzed by a dimeric gold complex. *Org. Lett.* **22**, 5844–5849 (2020).
24. Sahoo, B., Hopkinson, M. N. & Glorius, F. Combining gold and photoredox catalysis: visible light-mediated oxy- and aminoarylation of alkenes. *J. Am. Chem. Soc.* **135**, 5505–5508 (2013).
25. Liu, K. et al. Dinuclear gold-catalyzed C–H bond functionalization of cyclopropenes. *Sci. China Chem.* **64**, 1958–1963 (2021).
26. He, Y., Wu, H. & Toste, F. D. A dual catalytic strategy for carbon–phosphorus cross-coupling via gold and photoredox catalysis. *Chem. Sci.* **6**, 1194–1198 (2015).
27. Zhang, S., Wang, C., Ye, X. & Shi, X. Intermolecular alkene difunctionalization via gold-catalyzed oxyarylation. *Angew. Chem. Int. Ed.* **59**, 20470–20474 (2020).
28. Rodriguez, J. et al. Au(I)/Au(III) catalytic allylation involving π-allyl Au(III) complexes. *ACS Catal.* **12**, 993–1003 (2022).
29. Chintawar, C. C., Bhoyare, V. W., Mane, M. V. & Patil, N. T. Enantioselective Au(I)/Au(III) redox catalysis enabled by chiral (P, N)-ligands. *J. Am. Chem. Soc.* **144**, 7089–7095 (2022).
30. Yuan, T. et al. Alkyne trifunctionalization via divergent gold catalysis: combining π-acid activation, vinyl-gold addition, and redox catalysis. *J. Am. Chem. Soc.* **143**, 4074–4082 (2021).
31. Li, J. et al. switchable divergent synthesis in gold-catalyzed difunctionalizations of *o*-alkynylbenzenesulfonamides with aryldiazonium salts. *Org. Lett.* **23**, 7713–7717 (2021).
32. Peng, H., Cai, R., Xu, C., Chen, H. & Shi, X. Nucleophile promoted gold redox catalysis with diazonium salts: C–Br, C–S and C–P bond formation through catalytic sandmeyer coupling. *Chem. Sci.* **7**, 6190–6196 (2016).
33. Thirumurugan, P., Matosiuk, D. & Jozwiak, K. Click chemistry for drug development and diverse chemical–biology applications. *Chem. Rev.* **113**, 4905–4979 (2013).
34. Chinchilla, R. & Nájera, C. Recent advances in Sonogashira reactions. *Chem. Soc. Rev.* **40**, 5084–5121 (2011).
35. Sonogashira, K., Tohda, Y. & Hagihara, N. A convenient synthesis of acetylenes: catalytic substitutions of acetylenic hydrogen with bromoalkenes, iodoarenes and bromopyridines. *Tetrahedron Lett.* **16**, 4467–4470 (1975).
36. Bhoyare, V. W., Tathe, A. G., Das, A., Chintawar, C. C. & Patil, N. T. The interplay of carbophilic activation and Au(I)/Au(III) catalysis: an emerging technique for 1,2-difunctionalization of C–C multiple bonds. *Chem. Soc. Rev.* **50**, 10422–10450 (2021).
37. De Haro, T. & Nevado, C. Gold-catalyzed ethynylation of arenes. *J. Am. Chem. Soc.* **132**, 1512–1513 (2010).
38. Banerjee, S., Ambegave, S. B., Mule, R. D., Senthilkumar, B. & Patil, N. T. Gold-catalyzed alkynylative Meyer–Schuster rearrangement. *Org. Lett.* **22**, 4792–4796 (2020).
39. Brand, J. P. & Waser, J. Para-selective gold-catalyzed direct alkynylation of anilines. *Org. Lett.* **14**, 744–747 (2012).
40. Brand, J. P., Charpentier, J. & Waser, J. Direct alkynylation of indole and pyrrole heterocycles. *Angew. Chem. Int. Ed.* **48**, 9346–9349 (2009).
41. Szekely, A., Peter, A., Aradi, K., Tolnai, G. L. & Novak, Z. Gold-catalyzed direct alkynylation of azulenes. *Org. Lett.* **19**, 954–957 (2017).
42. Hofer, M., De Haro, T., Gomez-Bengoa, E., Genoux, A. & Nevado, C. Oxidant speciation and anionic ligand effects in the gold-catalyzed oxidative coupling of arenes and alkynes. *Chem. Sci.* **10**, 8411–8420 (2019).
43. Kim, S., Rojas-Martin, J. & Toste, F. D. Visible light-mediated gold-catalysed carbon($sp^2$)–carbon($sp$) cross-coupling. *Chem. Sci.* **7**, 85–88 (2016).
44. Tlahuext-Aca, A., Hopkinson, M. N., Sahoo, B. & Glorius, F. Dual gold/photoredox-catalyzed C($sp$)–H arylation of terminal alkynes with diazonium salts. *Chem. Sci.* **7**, 89–93 (2016).
45. Cai, R. et al. Ligand-assisted gold-catalyzed cross-coupling with aryldiazonium salts: redox gold catalysis without an external oxidant. *Angew. Chem. Int. Ed.* **54**, 8772–8776 (2015).
46. Wu, Y. et al. Electrochemical palladium-catalyzed oxidative Sonogashira carbonylation of arylhydrazines and alkynes to ynones. *J. Am. Chem. Soc.* **143**, 12460–12466 (2021).
47. Jiao, K. J., Xing, Y. K., Yang, Q. L., Qiu, H. & Mei, T. S. Site-selective C–H functionalization via synergistic use of electrochemistry and transition metal catalysis. *Acc. Chem. Res.* **53**, 300–310 (2020).
48. Wang, H., Gao, X., Lv, Z., Abdelilah, T. & Lei, A. Recent advances in oxidative $R^1$–H/$R^2$–H cross-coupling with hydrogen evolution via photo-/electrochemistry. *Chem. Rev.* **119**, 6769–6787 (2019).
49. Malapit, C. A. et al. Advances on the merger of electrochemistry and transition metal catalysis for organic synthesis. *Chem. Rev.* **122**, 3180–3218 (2022).
50. Ackermann, L. Metalla-electrocatalyzed C–H activation by earth-abundant 3d metals and beyond. *Acc. Chem. Res.* **53**, 84–104 (2020).
51. Huang, B., Sun, Z. & Sun, G. Recent progress in cathodic reduction-enabled organic electrosynthesis: trends, challenges, and opportunities. *eScience* **2**, 243–277 (2022).
52. Cheng, X. et al. Recent applications of homogeneous catalysis in electrochemical organic synthesis. *CCS Chem.* **4**, 1120–1152 (2022).

53. Ma, C. et al. Recent advances in organic electrosynthesis employing transition metal complexes as electrocatalysts. *Sci. Bull.* **66**, 2412–2429 (2021).
54. Ye, X. et al. Facilitating gold redox catalysis with electrochemistry: an efficient chemical-oxidant-free approach. *Angew. Chem. Int. Ed.* **58**, 17226–17230 (2019).
55. Zhang, S., Ye, X., Wojtas, L., Hao, W. & Shi, X. Electrochemical gold redox catalysis for selective oxidative arylation. *Green Synth. Catal.* **2**, 82–86 (2021).
56. Xie, J. et al. Light-induced gold-catalyzed Hiyama arylation: a coupling access to biarylboronates. *Angew. Chem. Int. Ed.* **57**, 16648–16653 (2018).
57. Witzel, S., Hashmi, A. S. K. & Xie, J. Light in gold catalysis. *Chem. Rev.* **121**, 8868–8925 (2021).
58. Xia, S. & Xie, J. Energy transfer in gold photocatalysis. *Gold Bull.* **55**, 123–127 (2022).
59. Lin, B. et al. Gold-catalyzed desymmetric lactonization of alkynylmalonic acids enabled by chiral bifunctional P,N ligands. *Angew. Chem. Int. Ed.* **61**, e202201739 (2022).
60. Yang, W. L., Shang, X. Y., Luo, X. & Deng, W. P. Enantioselective synthesis of spiroketals and spiroaminals via gold and iridium sequential catalysis. *Angew. Chem. Int. Ed.* **61**, e202203661 (2022).
61. Lin, X. et al. Biomimetic approach to the catalytic enantioselective synthesis of tetracyclic isochroman. *Nat. Commun.* **12**, 4958 (2021).
62. Zhang, M., Xie, J. & Zhu, C. A general deoxygenation approach for synthesis of ketones from aromatic carboxylic acids and alkenes. *Nat. Commun.* **9**, 3517 (2018).
63. Huang, H., Zhang, G., Gong, L., Zhang, S. & Chen, Y. Visible-light-induced chemoselective deboronative alkynylation under biomolecule-compatible conditions. *J. Am. Chem. Soc.* **136**, 2280–2283 (2014).
64. Anhauser, L., Teders, M., Rentmeister, A. & Glorius, F. Bio-additive-based screening: toward evaluation of the biocompatibility of chemical reactions. *Nat. Protoc.* **14**, 2599–2626 (2019).
65. Hashmi, A. S. K. et al. Simple gold-catalyzed synthesis of benzofulvenes—*gem*-diaurated species as 'instant dual-activation' precatalysts. *Angew. Chem. Int. Ed.* **51**, 4456–4460 (2012).


## Acknowledgements

We thank the National Natural Science Foundation of China (22122103 and 21971108 to J.X.), National Key Research and Development Program of China (2021YFC2101901 and 2022YFA15032 to J.X.), Fundamental Research Funds for the Central Universities (020514380252, 020514380272 to J.X.) and China Postdoctoral Science Foundation (2020TQ0139 and 2021M701661 to C.-G.Z.) for financial support. We acknowledge Xu Cheng at Nanjing University for insightful discussion and assistance. All theoretical calculations were performed at the High-Performance Computing Center of Nanjing University. We also acknowledge Yaohang Cheng, Yantao Li and Nian Li at Nanjing University for reproduction of the experimental procedures for products **4**, **33** and **39**.

## Author contributions

J.X. and H.L. conceived of and designed the project. H.L., Y.J. and C.-G.Z. performed and analysed the experimental data. J.X. wrote the manuscript with input from all authors.

## Competing interests

The authors declare no competing interests.

## Additional information

**Supplementary information** The online version contains supplementary material available at https://doi.org/10.1038/s44160-022-00219-w.

**Correspondence and requests for materials** should be addressed to Jin Xie.

**Peer review information** *Nature Synthesis* thanks Huan-Ming Huang, Xiaodong Shi and the other, anonymous, reviewer(s) for their contribution to the peer review of this work. Primary Handling Editor: Peter Seavill, in collaboration with the *Nature Synthesis* team.